

Accurate Bulk Properties from Approximate Many-Body Techniques

Judith Harl and Georg Kresse

Faculty of Physics, Universität Wien, and Center for Computational Materials Science, Sensengasse 8/12, A-1090 Wien, Austria
(Received 2 April 2009; published 29 July 2009)

For *ab initio* electronic structure calculations, the random-phase approximation to the correlation energy is supposed to be a suitable complement to the exact exchange energy. We show that lattice constants, atomization energies of solids, and adsorption energies on metal surfaces evaluated using this approximation are in very good agreement with experiment. Since the method is fairly efficient and handles ionic, metallic, and van der Waals bonded systems equally well, it is a very promising choice to improve upon density functional theory calculations, without resorting to more demanding diffusion Monte Carlo or quantum chemical methods.

DOI: 10.1103/PhysRevLett.103.056401

PACS numbers: 71.15.Nc, 31.10.+z, 71.10.-w, 71.45.Gm

The many electron Schrödinger equation lies at the heart of computational quantum chemistry, solid state physics, and materials science, but unfortunately, the computational complexity of the equation increases exponentially with the number of particles. Scientists are faced with the problem of finding accurate, but still tractable, methods for approximating the Schrödinger equation. The most favored method is presently density functional theory (DFT) [1]. While formally scaling as N^3 (where N characterizes the system size), the computational costs often increase only linearly for extended systems. Regrettably, we have seen little progress in the development of DFT functionals in recent years, with only incremental advances since the seminal work of Becke and Perdew in the early 1990s [2–4], when generalized gradient corrections (GC) and hybrid functionals that include a fixed fraction of exact exchange were introduced. The most common practice to mitigate the approximate nature of the available functionals is to devise specialized DFT parametrizations that work well for a selected class of problems, e.g., suitable gradient corrected functionals accounting well for the lattice constants and elastic properties of solids [5–7] or the aforementioned hybrid functionals [8] describing most semiconductors outstandingly well. Unfortunately, these methods tend to worsen the description of other properties, in the previous two cases, for instance, the description of adsorption on metal surfaces [9]. Another problem not addressed by GCs and hybrid functionals is the intrinsic nonlocal nature of correlation, leading to long-range van der Waals and Casimir forces [10]. Promising functionals that handle this type of problem are presently developed, but they are still in their infancy and so far show only moderate success [11]. The question emerges whether we really need to deal with all the complexity of the many electron Schrödinger equation as it is done in the diffusion Monte Carlo method [12] or some quantum chemistry methods such as the coupled cluster approach [13]. It goes without saying that these methods scale much worse than DFT, e.g., at least like N^4 (fixed-node diffusion

Monte Carlo method) or N^7 [coupled cluster singles, doubles, and perturbative triples [CCSD(T)]].

Any “good” approximate method should incorporate (i) in a materials dependent fashion a screened nonlocal exchange term and (ii) long-range dynamic correlation effects. Hybrid functionals with fixed exact exchange are a step in the right direction, and locally adjusting the amount of exact exchange can be a solution to (i) [14]. Remarkably, a simple approximation to achieve both goals has been known since at least 1958 [15]: the random-phase approximation (RPA) to the correlation energy. The expression can be derived in many different ways, from many-body Green function theory [16,17], using the adiabatic-connection fluctuation-dissipation theorem (ACFDT) [18,19], or from coupled cluster theory [20,21]. Despite its promising features, the method has not been applied systematically to extended systems, and there is no consensus whether the RPA improves upon available density functionals. Since efficient RPA implementations have become increasingly available for solids [22–24] and molecular systems [21,25–27], it is timely to access the overall quality of the RPA for solids and their surfaces.

Our implementation relies on the ACFDT inspired formulation of the RPA correlation energy. Neglecting any exchange-like terms in the correlation energy E_c yields (Coulomb or direct RPA)

$$E_c = \int_0^\infty \frac{d\omega}{2\pi} \text{Tr}[\ln(1 - \chi^0(i\omega)v) + \chi^0(i\omega)v], \quad (1)$$

where the trace (Tr), the independent particle response function χ^0 , and the Coulomb kernel v are evaluated in a suitable basis (plane waves in our case) at complex frequencies $i\omega$ (methodological details are discussed in Ref. [24]). The matrix operations in Eq. (1) scale like N^3 , whereas the evaluation of the response function requires at most N^4 operations [24], although N^3 algorithms are known [28]. This establishes that the method is in principle favorably scaling. In practice, the evaluation of

the response function is the main computational task, but our present implementation achieves peak performance and reaches a parallel efficiency of 90% on 100 CPU cores.

The independent particle response function, the correlation energy E_c , and the exact exchange energy (EXX) E_{EXX} (Hartree-Fock energy) are *all* evaluated using Kohn-Sham (KS) orbitals to yield the total ground-state energy $E = E_{\text{EXX}} + E_c$. All calculations presented here were performed using the VASP code and suitably optimized projector augmented wave (PAW) potentials that describe high energy scattering properties very accurately up to 100 eV above the vacuum level [29]. Only valence orbitals were included in the calculation of the correlation energy, whereas all orbitals were included in the EXX energy. Tests performed by unfreezing core states or changing the construction of the PAW potentials indicate that the lattice constants are technically accurate to at least 0.2%–0.3% and cohesive energies to about 2%. Our calculations are fully converged with respect to the k points, energy cutoffs, and with respect to the number of virtual orbitals and follow the same strategy as outlined in Ref. [24]. More details will be presented elsewhere [30].

Figure 1 shows the lattice constants for selected systems, including ionic systems, semiconductors, and metals. As a reference we also show local-density approximation (LDA) and Perdew-Burke-Ernzerhof (PBE) [4] results, as well as EXX results. The RPA and the EXX energies are calculated using PBE orbitals, but results for the lattice constants are practically identical for LDA orbitals. Since the orbitals were not determined self-consistently for the EXX case, the only difference between the EXX and the RPA result is the inclusion of the correlation energy in the RPA. As expected, LDA seriously underestimates the lattice constants [mean relative error (MRE) -1.5%], whereas PBE overestimates the lattice constants (MRE 0.9%). The PBE overestimation generally increases with

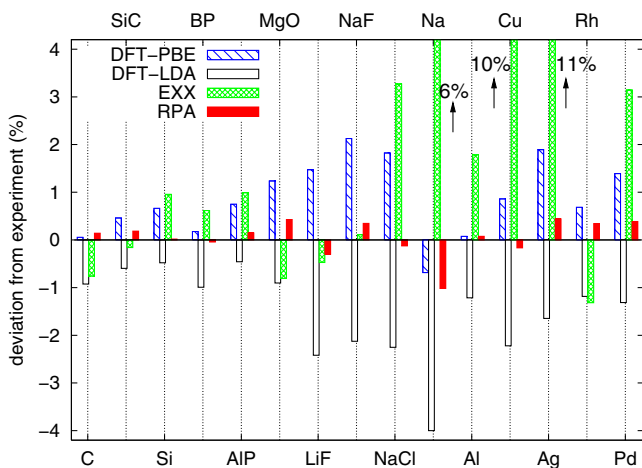


FIG. 1 (color online). Relative error (%) of the theoretical lattice constants of insulators, semiconductors, and metals. The experimental lattice constants are summarized in Ref. [33] and have not been corrected for zero-point vibrational effects.

increasing mass (e.g., $C \rightarrow Si$, $BP \rightarrow AlP$), as also observed in larger data sets [31]. EXX performs well for covalently bonded systems, but errors show more scatter around experiment than for DFT. Furthermore, the EXX approximation exhibits huge errors for metals, with only Rh, an open shell $4d$ metal, being an exception (covalent $4d-4d$ interaction). Bonding in metals and ionic systems with heavier elements is clearly not handled well in the EXX approximation. A self-consistent Hartree-Fock treatment does not change this trend.

Inclusions of correlation in the RPA remedies these problems entirely. In particular, for those materials where EXX was yielding too small lattice constants, the lattice constants increase (C, MgO, and Rh), whereas usually RPA decreases them. The improvements for NaCl and the metals are in fact little short of spectacular. Note again that our treatment includes full exact exchange, and RPA is the only “simple” but nonlocal correlation functional curing the shortcomings of EXX [32].

The atomization energies shown in Fig. 2 confirm our previous observations. The importance of correlation increases with increasing polarizability [compare Eq. (1)]: for the strongly polarizable metals correlation accounts for more than 80% of the atomization energy, whereas weakly polarizable insulators are well approximated by EXX. It is remarkable that the results for open shell transition metals are not much worse than for other metals, indicating that the RPA correlation is a good approximation even for systems that are considered to have at least some multi-determinantal character. This suggests that the ground states of the Pd and Rh metals are dominated by a single Slater determinant, which is well represented by the Kohn-Sham orbitals, dressed by double excited Slater determinants, as assumed in the RPA.

However, even after inclusion of the RPA correlation energy, the errors in the atomization energies remain fairly large and amount to about 0.2–0.4 eV. This is worse than

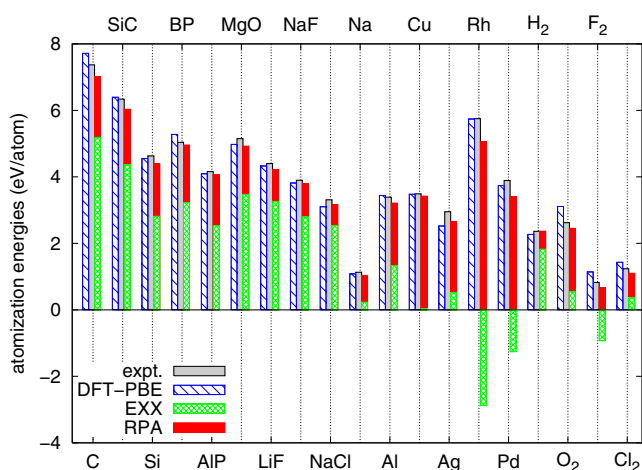


FIG. 2 (color online). Atomization energies (eV/atom) evaluated from EXX and RPA, compared to experimental and DFT-PBE values.

TABLE I. Heats of formation at $T = 0$ K in kJ/mol (per formula unit) with respect to the elemental phases in their normal state under ambient conditions. Experimental values are collected in Ref. [33], if not otherwise stated, and have been corrected for zero-point vibrations (ZPV) (experimental values without corrections are in parentheses). The ZPV have been evaluated using harmonic *ab initio* phonon calculations.

Solid	PBE	LDA	EXX	RPA	Expt.
LiF ^a	570	613	664	609	619 (614)
NaF	522	558	607	567	577 (573)
NaCl	355	381	433	405	413 (411)
MgO ^a	516	595	587	577	604 (597)
MgH ₂ ^a	52	89	113	72	78 (68)
AlN	262	327	350	291	321 (313 ^b)
SiC	51	54	69	64	69 (72)

^abcc Li, hcp Mg, and rutile MgH₂ were considered in their experimental geometries, whereas for the other materials the theoretical minimum energy geometries were used.

^bRef. [34].

for the PBE functional, which sometimes overestimates and sometimes underestimates the atomization energies, but gives a slightly smaller mean relative error. Similar results were found for small molecules [25] (see also H₂-Cl₂ results in Fig. 2). Hence, as a further benchmark, we have evaluated the heats of formation for a small set of systems, summarized in Table I. For the RPA, the formation energies agree well with experiment with similar or smaller errors than for the atomization energies, suggesting partial error cancellation. This is contrary to PBE, which severely underbinds as a consequence of the overbinding of the dimolecular species, whereas EXX yields too large formation energies for the considered solids, since the metals are too weakly bound. Astonishingly, LDA performs almost on par with RPA, although it yields too large atomization energies. In summary, among the considered approximations, RPA seems to be best balanced with a general slight tendency towards underbinding (atomization energies, heats of formation, and lattice constants).

van der Waals bonded rare-gas solids have been considered in Ref. [24]. To determine how well the RPA handles energy differences between covalent and van der Waals bonded systems, we show the atomization energy of graphite and diamond in Fig. 3. The first thing to note is that the RPA predicts a $1/d^4$ behavior for the graphite-graphite interlayer interaction (inset), as expected for van der Waals interactions between sheets at medium range [35], whereas neither EXX nor LDA and PBE are able to describe the interaction even qualitatively. After adding zero point corrections (11 meV in favor of graphite), RPA predicts graphite and diamond to be exactly degenerate in energy, whereas in experiment the graphite structure is found to be more stable by ≈ 5 –20 meV. PBE and EXX perform significantly worse, and incorrectly predict diamond to be more stable by 140 and 180 meV (zero point corrected), respectively.

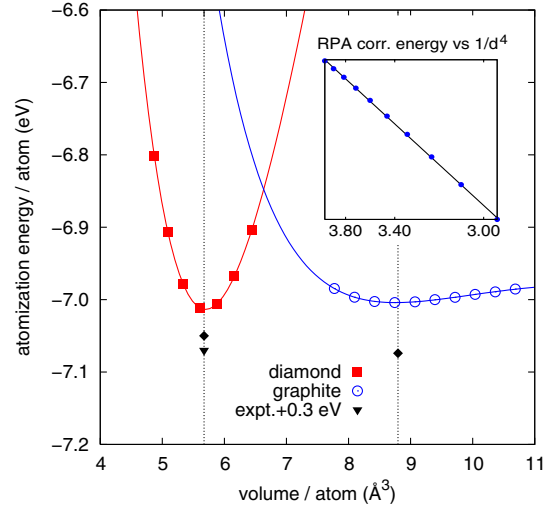


FIG. 3 (color online). RPA atomization energy (eV/atom) of diamond and graphite versus volume/atom. The experimental equilibrium volumes and atomization energies are indicated by black diamonds and black triangles. The experimental values are shifted upwards by 0.3 eV. The inset shows the RPA correlation energy of graphite versus $1/d^4$, where d is the graphite interlayer distance.

As a representative surface science problem, we have considered the interaction of CO with the Cu(111) surface (Table II), where PBE yields too large adsorption energies and the wrong site order, i.e., preference of the threefold coordinated fcc site, whereas experiments clearly point towards adsorption on top of a Cu atom [9,37,38]. Using EXX only, we find no binding, whereas the RPA not only predicts adsorption energies in good agreement with experiment and high level quantum chemistry calculations (CASPT2) but also recovers the correct site order [37].

In summary, for all cases we have yet considered, EXX + RPA is surpassing traditional density functionals. It is important to understand why the RPA is fairly reliable, and when we expect it to break down. The gist of RPA is to approximate the response function of the interacting many electron system by [25,39]

$$\chi^{\text{RPA}} = \chi^0 + \chi^0 \nu \chi^0 + \chi^0 \nu \chi^0 \nu \chi^0 + \dots \quad (2)$$

This is equivalent to including only direct symmetric terms (bubbles or ring diagrams) in the diagrammatic expansion of the correlation energy [17,21]. Consequently, the bare

TABLE II. CO adsorption energy on Cu(111) for a 2×2 supercell with 4 layers. A cluster based RPA approach yields -0.35 eV for atop adsorption [27].

	PBE	EXX	RPA	CASPT2 ^b	Expt. ^a
Top	-0.68	≈ 0.90	-0.42	-0.49	-0.49
fcc	-0.82	≈ 1.80	-0.30	>0	

^aRef. [36].

^bRef. [37].

exchange interaction is replaced by a frequency dependent screened exchange interaction [$v \rightarrow v(1 + \chi^{\text{RPA}}v)$] [16]. The main reason for the success must be that the RPA response function χ^{RPA} evaluated using KS orbitals captures important features of the “real” many-body interacting response function. This agreement can only be partial, since DFT gives unreliable results for the optical transition energies [poles in $\chi(\omega)$], but these are not directly relevant for the correlation energy, which is hinted at by the complex frequency integration in Eq. (1). In fact, using KS orbitals, the RPA reproduces static experimental polarizabilities quite well, essentially because static properties are ground-state properties. We have argued that this is the main reason why quasiparticle energies are so well approximated using the RPA G_0W_0 approximation [40], and obviously the same applies to correlation energies. The most serious remaining shortcoming is that the RPA neglects all antisymmetric terms in the diagrammatic expansion of E_c and is therefore not self-correlation free. Although the self-correlation error seems to drop out, in particular for heats of formation and lattice constants and to a lesser extent for atomization energies, the antisymmetric terms reduce the absolute correlation energies by about 30% [20]. One can attempt to approximate these terms by a local approximation as done in the RPA+, but in practice, we and others [25] found the RPA+ to worsen agreement with experiment. Explicitly evaluating these terms is a very expensive, but much better approximation, which makes the RPA self-correlation free and generally increases the binding and resultantly cures the main errors of the RPA [41].

In conclusion, we expect the RPA correlation energies to be reliable if the static RPA polarizabilities are. This covers a large range of solid state and molecular systems. The method applied here is a serious contender for routine calculations between traditional DFT methods and full quantum Monte Carlo calculations. Since it seamlessly incorporates van der Waals interactions, but also describes ionic bonding, covalent and metallic bonding, including d metal bonding, it is universally applicable to solids, molecules, and biological systems. The RPA might also be suitable for a numerical description of Casimir forces at short distances where microscopic details matter. Furthermore, we hope this work inspires the development of more approximate nonlocal density functionals that rely on a description of the correlation energy in the RPA.

This work was supported by the Austrian Fonds zur Förderung der wissenschaftlichen Forschung.

-
- [1] W. Kohn and L. J. Sham, Phys. Rev. **140**, A1133 (1965).
 - [2] A. D. Becke, Phys. Rev. A **38**, 3098 (1988).
 - [3] A. D. Becke, J. Chem. Phys. **98**, 5648 (1993).
 - [4] J. P. Perdew, K. Burke, and M. Ernzerhof, Phys. Rev. Lett. **77**, 3865 (1996).

- [5] R. Armiento and A. E. Mattsson, Phys. Rev. B **72**, 085108 (2005).
- [6] A. E. Mattsson *et al.*, J. Chem. Phys. **128**, 084714 (2008).
- [7] J. P. Perdew *et al.*, Phys. Rev. Lett. **100**, 136406 (2008).
- [8] A. V. Krukau, O. A. Vydrov, A. F. Izmaylov, and G. E. Scuseria, J. Chem. Phys. **125**, 224106 (2006).
- [9] A. Stroppa and G. Kresse, New J. Phys. **10**, 063020 (2008).
- [10] H. B. G. Casimir, D. Polder, Phys. Rev. **73**, 360 (1948).
- [11] M. Dion *et al.*, Phys. Rev. Lett. **92**, 246401 (2004).
- [12] W. M. C. Foulkes, L. Mitas, R. J. Needs, and G. Rajagopal, Rev. Mod. Phys. **73**, 33 (2001).
- [13] J. Cizek, Adv. Chem. Phys. **14**, 35 (1969).
- [14] A. V. Krukau, G. E. Scuseria, J. P. Perdew, and A. Savin, J. Chem. Phys. **129**, 124103 (2008).
- [15] P. Nozières and D. Pines, Phys. Rev. **111**, 442 (1958).
- [16] L. Hedin, Phys. Rev. **139**, A796 (1965).
- [17] N. E. Dahlen, R. van Leeuwen, and U. von Barth, Phys. Rev. A **73**, 012511 (2006).
- [18] O. Gunnarsson and B. I. Lundqvist, Phys. Rev. B **13**, 4274 (1976).
- [19] D. C. Langreth and J. P. Perdew, Solid State Commun. **17**, 1425 (1975); Phys. Rev. B **15**, 2884 (1977).
- [20] D. L. Freeman, Phys. Rev. B **15**, 5512 (1977).
- [21] G. E. Scuseria, T. M. Henderson, and D. C. Sorensen, J. Chem. Phys. **129**, 231101 (2008).
- [22] T. Miyake *et al.*, Phys. Rev. B **66**, 245103 (2002).
- [23] A. Marini, P. García-González, and A. Rubio, Phys. Rev. Lett. **96**, 136404 (2006).
- [24] J. Harl and G. Kresse, Phys. Rev. B **77**, 045136 (2008).
- [25] F. Furche, Phys. Rev. B **64**, 195120 (2001).
- [26] F. Furche, J. Chem. Phys. **129**, 114105 (2008).
- [27] X. Ren, P. Rinke, and M. Scheffler, Phys. Rev. B **80**, 045402 (2009).
- [28] H. N. Rojas, R. W. Godby, and R. J. Needs, Phys. Rev. Lett. **74**, 1827 (1995).
- [29] M. Shishkin and G. Kresse, Phys. Rev. B **74**, 035101 (2006).
- [30] J. Harl and G. Kresse (to be published).
- [31] F. Tran, R. Laskowski, P. Blaha, and K. Schwarz, Phys. Rev. B **75**, 115131 (2007).
- [32] J. P. Perdew, Int. J. Quantum Chem. **48**, 93 (1993).
- [33] J. Paier *et al.*, J. Chem. Phys. **127**, 024103 (2007).
- [34] D. D. Wagman *et al.*, J. Phys. Chem. Ref. Data **11**, Suppl. 2, 1 (1982).
- [35] J. F. Dobson, A. White, and A. Rubio, Phys. Rev. Lett. **96**, 073201 (2006).
- [36] S. Vollmer, G. Witte, and C. Woell, Catal. Lett. **77**, 97 (2001).
- [37] S. Sharifzadeh, P. Huang, and E. Carter, J. Phys. Chem. C **112**, 4649 (2008).
- [38] Q.-M. Hu, K. Reuter, and M. Scheffler, Phys. Rev. Lett. **98**, 176103 (2007).
- [39] Y. M. Niquet, M. Fuchs, and X. Gonze, Phys. Rev. A **68**, 032507 (2003).
- [40] M. Shishkin, M. Marsman, and G. Kresse, Phys. Rev. Lett. **99**, 246403 (2007).
- [41] A. Grüneis, M. Marsman, and G. Kresse (to be published).